HOSTED BY
ELSEVIER
CrossMark
Available online at www.sciencedirect.com
ScienceDirect
Journal of Magnesium and Alloys 3 (2015) 16–22
www.elsevier.com/journals/journal-of-magnesium-and-alloys/2213-9567

Full length article

Investigation on mechanical properties and creep behavior of stir cast AZ91-SiC_p composites

Abhilash Viswanath [a], H. Dieringa [b], K.K. Ajith Kumar [a], U.T.S. Pillai [a,*], B.C. Pai [a]

[a] *CSIR – National Institute for Interdisciplinary Science and Technology, Material Science and Technology Division, Thiruvananthapuram 695019, India*
[b] *MagIC – Magnesium Innovation Centre, Helmholtz-Zentrum Geesthacht, Max-Planck-Strasse 1, D-21502 Geesthacht, Germany*

Received 1 September 2014; revised 1 January 2015; accepted 8 January 2015
Available online 6 March 2015

Abstract

The room temperature mechanical properties and high temperature creep behavior of AZ91 alloy reinforced with SiC_p synthesized via stir casting have been evaluated. The mechanical properties showed improvement with respect to the amount of reinforcement content. The creep testing of the composites carried out at a temperature of 175 °C under constant stress of 80, 100 and 120 MPa reveals different creep characteristics depending upon the reinforcement content and the applied load. The true stress exponents of different composites calculated from minimum creep rate indicate the possible mechanisms of creep deformation.

Keywords: Composites; Optical microscopy; Mechanical properties; Creep characteristics

1. Introduction

Being the lightest among the structural materials, magnesium based alloys have become a competent part in areas where weight reduction is among primary concerns [1]. Even though, structural components made of Mg alloys are plenty, load bearing Mg components, especially operating at higher temperature (>150 °C) are rare. Concerns over elevated temperature applications can be circumvented by developing Mg metal matrix composites (Mg MMC's) with reinforcements which are thermally stable. Also, these reinforcements strengthen the matrix by imparting better mechanical and tribological properties [2].

Among the various viable routes for the synthesis of Mg MMC's, pressure assisted infiltration (squeeze casting), pressure less infiltration, powder metallurgy and stir casting are the prominent ones. Infiltration processes (pressure less and pressure assisted) are capable of synthesizing composites with higher volume fraction of reinforcements; still, their applications are limited by the preform size [3]. Fine grained composites with near-uniform distribution of reinforcements along with highest possible reinforcement content can be produced via powder metallurgy route [4]. However, the restricted size of the composites and higher cost involved are the inherent disadvantages of this process. Even though, interfacial reaction is a major concern in stir casting, the process is considered as the most adaptable and economical route, due to its simplicity, flexibility, low processing cost and high production rate for synthesizing discontinuously reinforced composites [5].

As far as the thermal stability of the reinforcements are concerned, ceramic particles are the most desirable due to high level of hardness, strength and melting point. Among ceramic reinforcements used in Mg MMC, silicon carbide particles (SiC_p) are the most popular due to high stability and wettability in Mg matrix [2]. Furthermore, SiC_p reinforced Mg MMC's are reported with improved strength [6] and wear

* Corresponding author. Tel.: +91 471 2515236; fax: +91 471 2491712.
E-mail address: utspillai@rediff.com (U.T.S. Pillai).
Peer review under responsibility of National Engineering Research Center for Magnesium Alloys of China, Chongqing University.

http://dx.doi.org/10.1016/j.jma.2015.01.001.

resistance [7] than base alloys. However, investigations into high temperature creep properties of SiC_p reinforced composites with Mg matrix synthesized via stir casting are rare.

The present investigation aims to reveal the room temperature mechanical properties and high temperature creep properties of AZ91/SiC_p composite synthesized via stir casting. The creep testing of the composites has been performed by applying compressive loads as the stress applied in compressive manner represents real situations as in case of bolting of gear housing or parts of engine [8]. Stress exponents calculated from minimum creep rate reveal the mechanism of deformation involved.

2. Experimental

2.1. Composite preparation

About 1200 g of AZ91 (Mg-9.3Al-0.8Zn-0.18Mn) was used per casting as the matrix for preparing the composites. The alloy was melted in a steel crucible using a resistance heating furnace under protective atmosphere of argon gas. At the melt temperature of 750 °C, stirring was carried out using a steel impeller rotating at 750 rpm. The SiC_p having size ~23 μm was preheated to 600 °C and was added into the corner of the vortex during stirring. The amount of SiC_p corresponding to 5, 10, 15, 20 and 25% by weight of the matrix took about 10, 20, 30, 40 and 50 min respectively for the addition. The stirring was continued for 10 min after complete addition of SiC_p to ensure the mixing of reinforcement into the matrix. Subsequently, the melt was poured into a 300 °C preheated mild steel mould to obtain the castings.

2.2. Microstructure

The specimens for microscopy, obtained from the same area for all the castings to have comparable cases, were subjected to standard polishing using SiC abrasive papers and selvyte cloth with diamond paste. The polished specimens were etched with acetic picral etchant (5 ml acetic acid + 6 g picric acid + 10 ml H_2O + 100 ml ethanol). Leica DMRX optical microscope was used for the microstructural analysis. Microstructures with higher magnification were incurred using a scanning electron microscope (JEOL, JSM 35C) with an accelerating voltage of 15–30 keV.

2.3. Mechanical properties

Samples prepared according to ASTM E8 standard [9] were tested for room temperature tensile properties using a computer controlled INSTRON 8801 universal testing machine set with a cross head speed of 2 mm/min. The fractured surfaces of the tensile tested specimens were also examined under SEM.

2.4. Creep characteristics

Cylindrical specimens with length 15 mm and 6 mm diameter were used for compression creep tests. The specimens were tested at 175 °C under constant stresses of 80, 100 and 120 MPa using an ATS lever arm system.

3. Results and discussion

3.1. Microstructural observations and interfacial characteristics

The XRD analysis done for phase identification revealed the presence of the Mg matrix, the inherent intermetallic phase $Mg_{17}Al_{12}$ and the reinforcement SiC. The traces of oxide layer MgO along with Mg_2Si intermetallic phase are also detected. The details of the analysis have been published elsewhere [10].

Fig. 1 depicts the optical micrographs of AZ91 base alloy and AZ91-SiC_p composites with 5, 10, 15, 20 and 25 wt% SiC_p content. A typical two phase microstructure of AZ91 alloy with α-Mg phase and β-$Mg_{17}Al_{12}$ phase along and adjacent to the grain boundaries is shown in Fig. 1(a). Near-uniform distribution of SiC_p can be noted in microstructure of the composites depicted in Fig. 1 (b–f). Moreover, the reinforcements are found to be dispersed in the matrix with very few agglomerations. Generally, the increase in particle reinforcement content tends to increase the agglomeration in composites. This is attributed to the finer size of the reinforcements and variations in parameters like stirring time, stirring speed, stirring temperature, etc [11]. Moreover, noticeable presence of MgO in the form of white patches or that of Mg_2Si in needle like or dots cannot be evidenced in the microstructure as of XRD results. This nullifies the effect of such phases on formation of microstructure.

Moreover, the grain size is reduced from 65 microns for the base alloy to 34 microns for 5 wt% SiC_p containing composites and then to 22 microns for composite containing 10 wt % SiC_p. However, the grain size reduction is comparitively negligible for higher reinforcement containing composites i.e. 21 microns for 25 wt% SiC_p.

The possible refinement mechanism behind reduction in grain size of the matrix due to the presence of SiC_p is heterogeneous nucleation. The reinforcing SiC_p which can act as the heterogeneous nucleation site may get captured by growing Mg crystals and finally stay within the Mg grains in the composites. Hence, the presence of SiC_p within the grain boundaries of the composite is justified. Moreover, certain crystallographic orientation relationships between the particle and matrix and the restricted growth of Mg grains by SiC_p during solidification can further contribute to the reduction in grain size [11,12] which is evidenced by the presence of the reinforcements around the grains as clusters.

Interfacial reactions are of extreme importance while considering the mechanical and creep properties of the composite as the load transfer between the reinforcements and the matrix is governed by the interface between them. The SEM microstructure of AZ91-20SiC_p composite shown in Fig. 2a reveals good distribution of the particles. The high magnification SEM micrograph in Fig. 2b shows the intimate bonding of SiC_p with Mg matrix which nullifies the occurance of any significant chemical reaction at the Mg-SiC_p interfaces.

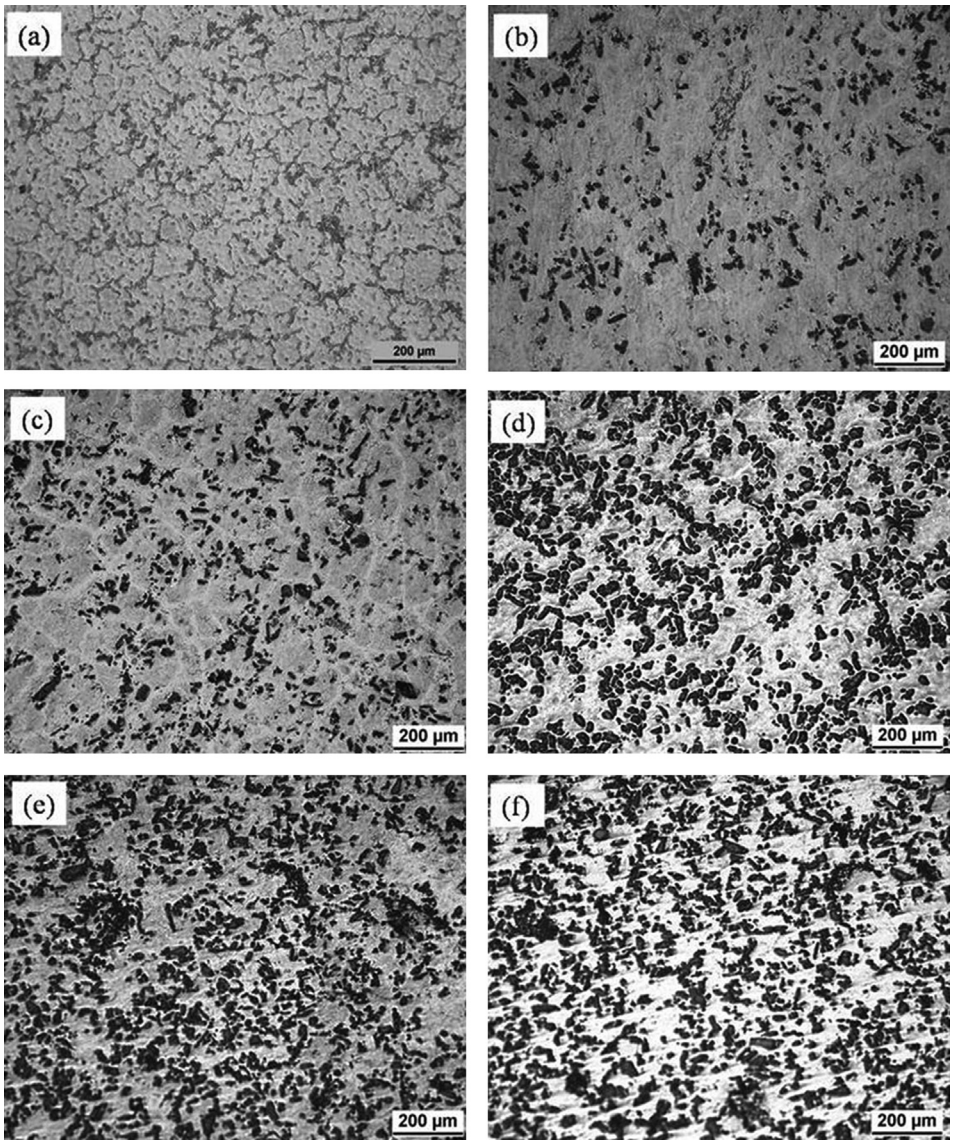

Fig. 1. Optical micrographs of AZ91 alloy with a) 0, b) 5, c) 10, d) 15 and e) 20 and f) 25 wt-% SiC_p content.

Moreover, the sharp and clean (precipitate and reaction free) interface also depicts good interfacial integrity of SiC_p with the matrix. Studies conducted on the feasibility of compo-cast AZ91/SiC composites had similar conclusion stating that SiC wetted well with Mg and Mg is a better host for SiC_p embedment than Al. Moreover, the presence of Al in the AZ91 alloy has tremendous influence in improving the wettability of SiC_p reinforcements [13].

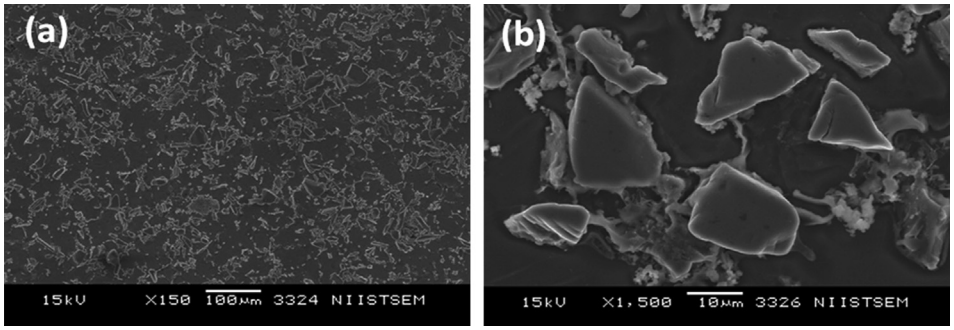

Fig. 2. SEM micrographs of a) AZ91-20SiC_p composite and b) Showing clean interface.

3.2. Mechanical properties and tensile fractography

The variation in yield strength (YS) and ultimate tensile strength (UTS) of AZ91 alloy with respect to the various SiC_p content is depicted as histogram in Fig. 3. The YS of the composites during tension shows a gradual increase with respect to the increment in amount of reinforcements. Studies pertaining to the tensile strength of Mg matrix composites have revealed that within a certain range, both yield strength and elastic modulus of the composites increase linearly with increase in amount of reinforcement. The key strengthening mechanisms in Mg matrix composites are particle strengthening, work hardening, load transfer and grain refinement of the matrix alloy by the reinforcement [2]. The finely dispersed SiC_p strengthen the Mg matrix by blocking the dislocation motion within the composites. Also, the smaller sized grains have improved strength within the elastic region and facilitate enhanced tensile properties for the composites at room temperature [14]. In the present composite system, the grain size reduction for AZ91-5SiC_p and AZ91-10SiC_p is more predominant compared with AZ91 alloy with 15, 20 and 25 wt% SiC_p. The variation in YS also depicts similar characteristics, with increment being high for 5 and 10 SiC_p containing composites as of composites with higher amount of reinforcing phase.

Moreover it is evident from the histogram that the improvement in strength during tension is limited to the elastic region, as the UTS of the composites do not show considerable variation from that of base alloy. The residual stress produced during the deformation process, failure of agglomerated submicron SiC_p and the presence little amount of porosity are the possible reasons behind constant levels of UTS of the composites.

The increase in ultimate tensile strength (UCS) of the composites (Fig. 4) is attributed to the presence of hard reinforcement particle which restrict the flow of dislocations in the matrix. Moreover, the compressive strength of the silicon carbide is very high (3900 MPa) compared to the base alloy value of 310 MPa. The significant increase in compressive strength observed in the composite can also be attributed to partial closure of the fine microscopic cracks during compression loading. Similar observation is also reported for SiC_p reinforced AZ92 Mg alloy composites [15].

The tensile fracture surfaces of the composites (Fig. 5 a and b) reveal both ductile and brittle mechanisms. The pockets like regions surrounding the fractured and deciphered SiC_p are termed as "tear ridges". These ridges are indicative of ductile failure and so are the pockets of dimples of varying size and shape in the fracture surface. The mechanical properties of the soft, ductile and elastically deforming AZ91 alloy matrix gets augmented by the hard, brittle and essentially plastically deforming reinforcing SiC_p. Moreover, the development of a resultant triaxial stress state in the matrix aids in limiting the flow stress of the composite [16]. Also, brittle fracture region increases with increase in SiC_p when compared to the ductile region.

3.3. Creep behavior

The increase in yield strength, ultimate compressive strength and the hardness is the motivation behind evaluation of creep properties. Mg alloys have an inherent disadvantage of relatively low creep resistance. The grain boundary slide and dislocation slip at both the basal and the non-basal planes results in high creep rate of Mg alloys [17]. Thus, incorporation of hard particles which can impede the grain boundry slide and the dislocation slip in the soft matrix can improve high temperature creep properties of Mg alloys.

Fig. 6 shows exemplarily creep curves of tests performed with AZ91-25SiC_p composite at a temperature of 175 °C with stress levels of 80, 100 and 120 MPa. The variation in creep deformation of the composite as a function of time for different applied loads depicted in Fig. 6a symbolizes a typical creep curve. The creep deformation increases with increase in

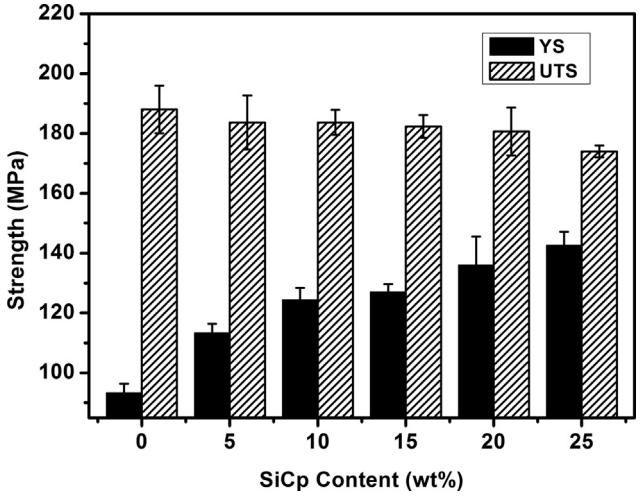

Fig. 3. Histogram showing variation in yield strength (YS) and ultimate tensile strength (UTS) of the composites with respect to SiC_p.

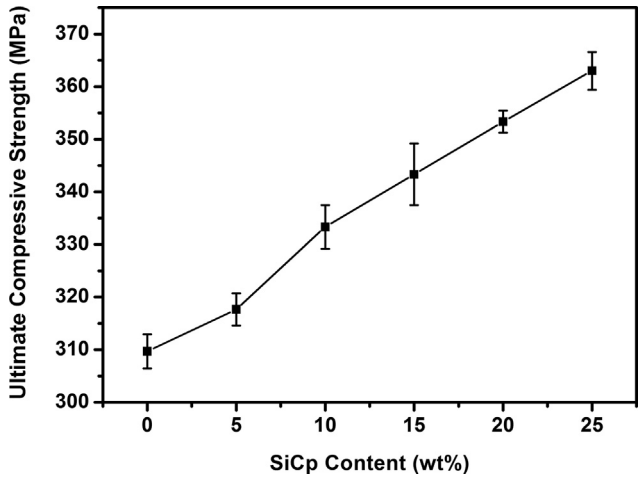

Fig. 4. Variation in ultimate compressive strength (UCS) of the AZ91 alloy with increase in reinforcement content.

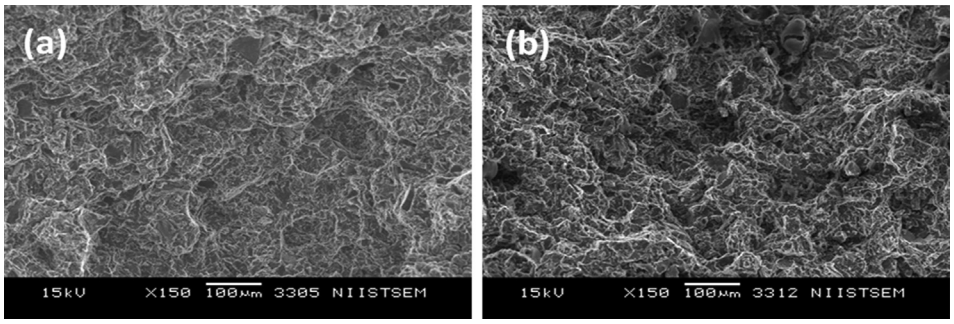

Fig. 5. SEM image of the fractured surface of the tensile tested specimens of a) AZ91/10 SiC_p and b) AZ91/20 SiC_p composites.

stress and associated time decreases as the load elevates. Hence, increase in applied stress reduces the test duration.

The creep rate of the composite is plotted against time for varying stress levels in Fig. 6b. The curves have similar characteristics with those from Fig. 6a in terms of variation of creep rate and time with respect to applied load. Moreover, reduction in minimum creep rate can also be evidenced with decreasing the applied load. The creep curves in Fig. 6c are the diagrammatical representation of the creep rate of the composite against its creep deformation under different loading conditions. It is clearly visible that minimum creep rate is reached in the first 10% of deformation and with increase in applied load, the deformation at which the minimum creep rate occurs, increases.

Creep deformation is the representation of the time dependant plastic flow occurring in crystalline and non-crystalline materials under an applied load which need not to be above the elastic limit of the material. Moreover, it is well documented that the classical creep curve of materials consists of three distinct stages namely primary stage in which

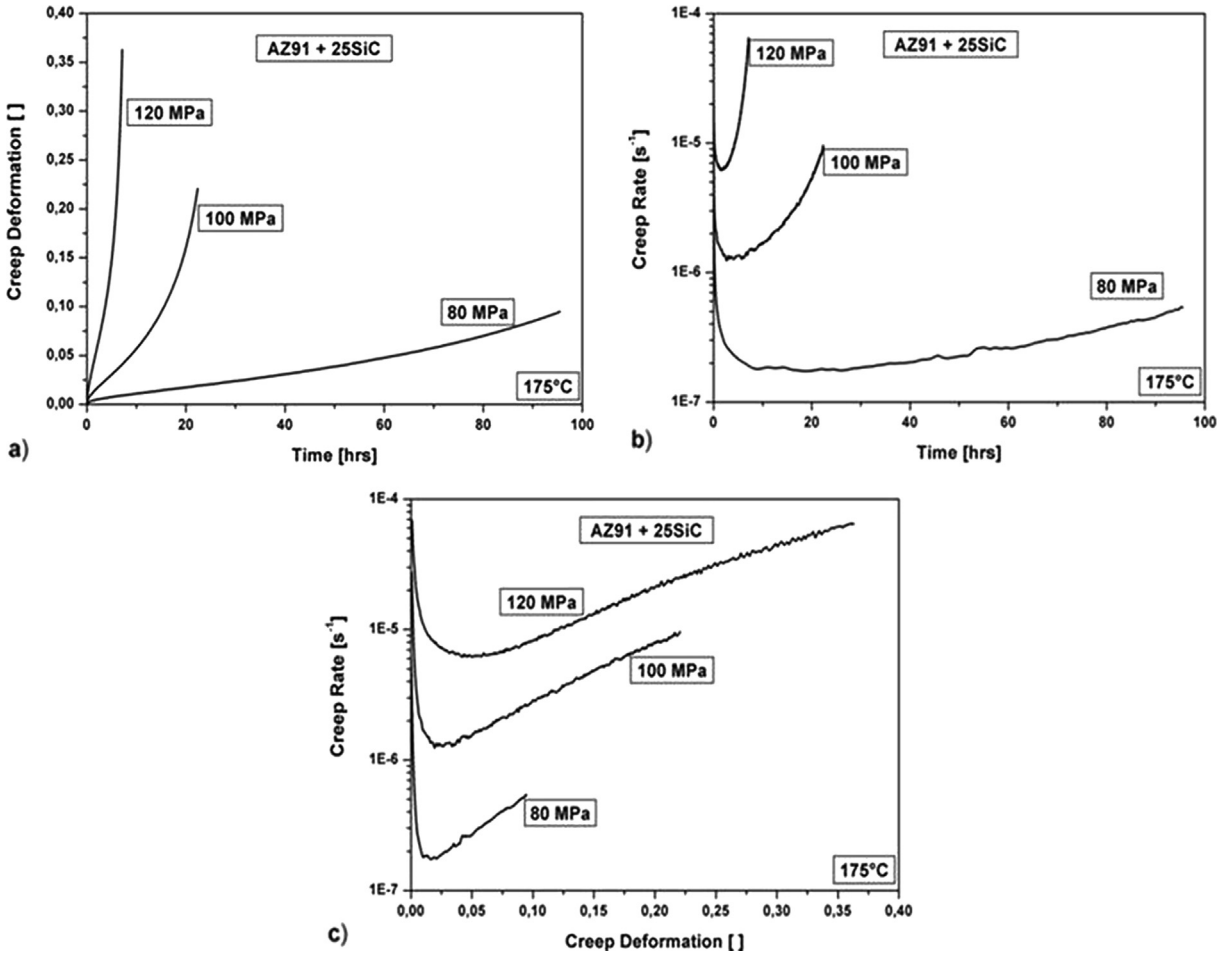

Fig. 6. Creep results of tests performed with AZ91 + 25SiC at 175 °C. a) Creep deformation over time, b) Creep rate over time and c) Creep rate over creep deformation from tests at applied stresses of 80, 100 and 120 MPa.

strain rate decreases with increase in time, a secondary stage where stain rate is reasonably constant and ternary stage where strain rate increases with time [18]. However, in the case of discontinuously reinforced composites, duration of secondary stage is relatively shorter. In such cases, the deformation mechanisms are best described using minimum creep rate which can be observed most readily in plots of creep rate against time [19].

The dependence of minimum creep rate $\dot{\varepsilon}_s$ on temperature and applied stress is given by the Norton-equation as:

$$\dot{\varepsilon}_s = \frac{ADGb}{kT}\left(\frac{\sigma}{G}\right)^n \quad (1)$$

where, A is a material dependent constant, G the shear modulus, b the Burgers vector, k the Boltzmann constant and n the stress exponent, D is the diffusion coefficient, which is

$$D = D_0 \cdot \exp^{(-Q_C/RT)}. \quad (2)$$

D_0 is the frequency factor and Q_C the activation energy for creep.

The stress exponent n gives information about rate-controlling deformation mechanisms during creep ($n = 3$ represents creep controlled by viscous glide [20], $n = 5$ is for creep controlled by high temperature climb of dislocation due to diffusion of the lattice [21], $n = 7$ symbolizes creep by low temperature climb of dislocation due to diffusion of the core [22], $n = 8$ is for lattice diffusion controlled creep deformation [23]).

The n values are determined by plotting the minimum creep rates in a double logarithmic plot versus stress field as shown in Fig. 7a. The filled squares in the graph represent AZ91 and the empty ones are those of the composites reinforced with different amounts of SiC_p. The base alloy and the composites with lower reinforcement content (5 and 10 wt %) evince less significant difference in minimum creep rates. However, the composites containing 15, 20 and 25 wt% SiC_p have an improved creep resistance. The calculated stress exponents n for the base alloy and composites are given in Table 1.

The values of stress exponent given in Table 1 shows variation in co-relation with the grain size and volume of reinforcements. For composites reinforced with thermally stable particles, the 'n' value naturally increases with increase in reinforcement content. However, in the present study, the 'n' value for AZ91-5SiC_p and AZ91-10SiC_p composites are very close to that of the base alloy. These alloys have phenomenally reduced grain size in comparison with composites with higher SiC_p content. For the composites with 15, 20 and 25 wt% SiC_p, the presence of elevated amount of reinforcement compensate for reduction in grain size, thus improving the stress exponent.

Table 1
Stress exponents, threshold stresses and true stress exponents of AZ91-SiC_p composites calculated from creep tests at 175 °C.

AZ91 with various wt-% SiC_p	0	5	10	15	20	25
Stress exponent (n)	7.2	7.4	7.7	8.5	8.4	8.9
Threshold stress (σ_{thr})	24.4	24.7	26.4	30.1	31.4	34.4
True stress exponent (n_t)	5.4	5.5	5.6	5.8	5.6	5.7

Studies have shown that in comparison with metals, the creep behavior of discontinuously reinforced alloys is unusual in two ways [24,25]. Firstly, the stress dependence of creep rate, as accounted by value of stress exponent 'n', is unnaturally high. Secondly, the temperature dependence of creep rate, usually measured as activation energy 'Q', is much larger than that for self-diffusion.

The high stress dependence of creep rate is due to the presence of threshold stress (σ_{thr}), the stress below which no creep deformation occurs, and is attributed to the interactions of the dislocation with the reinforcement. There are several explanations for threshold stress. It is often referred as the Orowan stress, which is the additional stress needed for bowing the dislocations between the reinforcements [26]. The σ_{thr} is also referred as the additional back stress which is required for climbing over an obstacle or as the stress needed for detaching dislocations from obstacles [27,28]. Hence, the stress term (σ) in eq (1) is to be replaced with the term of effective stress (σ_{eff}) to avoid the anomalous nature of the stress exponents. The equation gets modified as:

$$\dot{\varepsilon}_s = \frac{ADGb}{kT}\left(\frac{\sigma_{eff}}{G}\right)^{n_t} \quad (3)$$

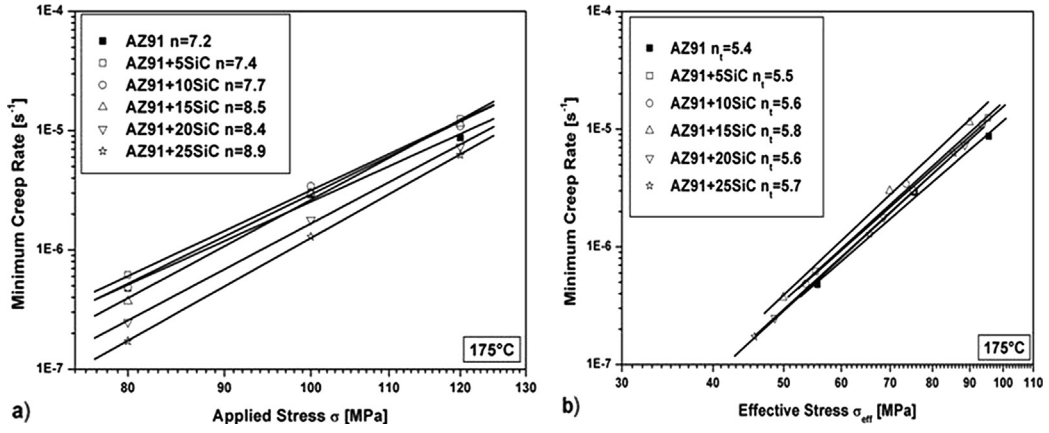

Fig. 7. Minimum creep rates as function of a) applied stress and b) effective stress for tests at 175 °C for AZ91 alloy with 0, 5, 10, 15, 20 and 25 wt-% SiC_p content.

where, $\sigma_{eff} = \sigma - \sigma_{thr}$ and n_t is the true stress exponent.

The estimation of values of threshold stress is done here using the method developed by Li and Langdon [29]. Each curve through the individual datum points are extrapolated to lie essentially vertical to a strain rate of $10^{-10}\,s^{-1}$, which corresponds to a deformation rate of approximately 1% in 3 years. The predicted stress levels at this low strain rate are very close to threshold stress. The double logarithmic plots of minimum creep rates versus the effective stress used for calculating true stress exponent is depicted in Fig. 7b. The calculated σ_{thr} values and associated true stress exponents are given in Table 1.

The true stress exponent values of the composites lie in the range of 5.4 and 5.8. As per literature, this can be attributed to the dislocation climbing at higher temperature [21,30].

4. Conclusions

Stir casting is an effective method for fabrication of AZ91-SiC_p composites with reinforcement content up to 25 wt-% and the reinforcements get near uniform distribution in the matrix with very less agglomeration and have cleaner interface. The grain size reduction in 5 and 10 SiC_p containing composites is high when compared with 15, 20 and 25 SiC_p containing composites and variation in mechanical and creep attributes are closely related with the same. The yield strength and ultimate compressive strength of the composites increases with increase in reinforcement content. But, the ultimate tensile strength remains comparable with that of the base alloy. The base alloy and the composites with lower reinforcement content (5 and 10 wt %) evince less significant difference in minimum creep rates. However, the composites containing 15, 20 and 25 wt% SiC_p have an improved creep resistance. As the true stress exponent values of the composites lie in the range of 5.4 and 5.8, the creep can be attributed to the dislocation climbing.

Acknowledgment

The authors are grateful to the Aeronautical Research and Development Board (ARDB), New Delhi for the financial grant for this work (GAP 214739). Mr. Prasanth Sujayakumar has been very helpful throughout the course of the work. The support received from Mr. K.K. Ravikumar for mechanical testing, Mr. M.R Chandran for SEM analysis and dedicated efforts from Mr. J.S Harikrishnan, Mr. K.A. Ajukumar and Mrs. K.S. Deepa, is also highly acknowledged.

References

[1] C. Blawert, N. Hort, K.U. Kainer, Trans. Indian Inst. Met. 57 (2004) 397–408.
[2] H.Z. Ye, X.Y. Liu, J. Mater. Sci. 39 (2004) 6153–6171.
[3] H. Lianxi, W. Erde, Mater. Sci. Eng. A 278 (2000) 267–271.
[4] B.W. Chua, L. Lu, M.O. Lai, Compo. Str. 47 (1999) 595–601.
[5] J. Hashim, L. Looney, M.S.J. Hashmi, J. Mater. Process. Technol. 92–93 (1999) 1–7.
[6] X.J. Wang, X.S. Hu, K.B. Nie, K. Wu, M.Y. Zheng, Trans. Nonfer. Met. Soc. China 22 (2012) 1912–1917.
[7] C.Y.H. Lim, S.C. Lim, M. Gupta, Wear 255 (2003) 629–637.
[8] H. Dieringa, Y. Huang, P. Maier, N. Hort, K.U. Kainer, Mater. Sci. Eng. A 410–411 (2005) 85–88.
[9] Standard test methods for tension testing of metallic materials http://enterprise1.astm.org/DOWNLOAD/E8-04.1203314-1.pdf.
[10] K.K. Ajith Kumar, A. Viswanath, T.P.D. Rajan, U.T.S. Pillai, B.C. Pai, Acta Metall. Sin. Engl. Lett. 27 (2014) 295–305.
[11] M.C. Gui, J.M. Han, P.Y. Li, J. Mater. Eng. Perform. 12 (2003) 128–134.
[12] P. Poddar, V.C. Srivastava, P.K. De, K.L. Sahoo, Mater. Sci. Eng. A 460–461 (2007) 357–364.
[13] A. Luo, Metall. Mater. Trans. A 26 (1995) 2445–2455.
[14] S. Pal, K.K. Ray, R. Mitra, Mater. Sci. Eng. A 527 (2010) 6831–6837.
[15] M. Jayamathy, S.V. Kailas, K. Kumar, S. Seshan, T.S. Srivatsan, Mater. Sci. Eng. A 393 (2005) 27–35.
[16] K. Manigandan, T.S. Srivatsan, T. Quick, Mater. Sci. Eng. A 534 (2012) 711–715.
[17] P. Lukac, Z. Trojanova, Z. Drozd, Key Eng. Mater. Dev. Light Metals 121–128 (2000).
[18] Z.Y. Ma, S.C. Tjong, Compo. Sci. Technol. 61 (2001) 771–786.
[19] F.A. Mohamed, K.T. Park, E.J. Lavernia, Mater. Sci. Eng. A 150 (1992) 21–35.
[20] F.A. Mohamed, T.G. Langdon, Acta. Metall. 22 (1974) 779–788.
[21] O.D. Sherby, P.M. Burke, Prog. Mater. Sci. 13 (1968) 323–390.
[22] S.L. Robinson, O.D. Sherby, Acta. Metall. 17 (1969) 109–125.
[23] O. Sherby, R. Klundt, A. Miller, Metall. Trans. A 8 (1977) 843–850.
[24] H.E. Evans, G. Knowles, Met. Sci. 14 (1980) 262–266.
[25] A.H. Clauer, N. Hansen, Acta. Metall. 32 (1984) 269–278.
[26] E. Orowan, Dislocations and mechanical properties, The American Institute of Mining and Metallurgical Engineering Inc, New York, 1954.
[27] E. Arzt, D.S. Wilkinson, Acta. Metall. 34 (1986) 1893–1898.
[28] E. Arzt, M.F. Ashby, Scr. Metall. 16 (1982) 1285–1290.
[29] Y. Li, T.G. Langdon, Scr. Mater. 36 (1997) 1457–1460.
[30] J. Weertman, J. Appl. Phys. 28 (1957) 1185–1189.